frontiers | Frontiers in Marine Science

TYPE Original Research
PUBLISHED 21 February 2025
DOI 10.3389/fmars.2025.1538734

OPEN ACCESS

EDITED BY
Lingshi Yin,
Hunan Agricultural University, China

REVIEWED BY
Mohamed Hamed,
Louisiana State University, United States
Wenrong Feng,
Chinese Academy of Fishery Sciences (CAFS), China

*CORRESPONDENCE
Guangpeng Feng
Fenggp@ecsf.ac.cn

RECEIVED 03 December 2024
ACCEPTED 31 January 2025
PUBLISHED 21 February 2025

CITATION
Xu J, Feng G and Yan Y (2025) Effects of polystyrene nanoplastics and copper on gill tissue structure, metabolism, and immune function of the Chinese mitten crab (*Eriocheir sinensis*).
Front. Mar. Sci. 12:1538734.
doi: 10.3389/fmars.2025.1538734

Effects of polystyrene nanoplastics and copper on gill tissue structure, metabolism, and immune function of the Chinese mitten crab (*Eriocheir sinensis*)

Jian Xu[1,2], Guangpeng Feng[1,2]* and Yunzhi Yan[2]

[1]Shanghai Yangtze Estuary Fishery Resources Proliferation and Ecological Restoration Engineering Technology Research Center, East China Sea Fisheries Research institute, Chinese Academy of Fishery Sciences, Shanghai, China, [2]School of Ecology and Environment, Anhui Normal University, Wuhu, China

Nanoplastics (NPs) and copper (Cu) are increasingly released into aquatic environments, posing significant risks to aquatic organisms, including crabs. As the primary interface between the organism and the surrounding environment, gills are particularly susceptible to the impacts of NPs and Cu exposure. Investigating the toxicity of these pollutants, especially their combined effects, is crucial for assessing their environmental risks. This study evaluated the toxicity of NPs (0.4 mg/L), Cu^{2+} (0.1 mg/L), and the combination (NPs + Cu^{2+}) on the gill tissues of *Eriocheir sinensis*, focusing on tissue morphology, metabolism, and immune functions. The results demonstrated that exposure to NPs, Cu^{2+} and NPs + Cu^{2+} caused structural damage to gill tissues and significantly elevated antioxidant parameters such as GSH-Px activity and GSH content, as well as immune parameters including ACP and AKP activity. Compared with the single exposure group, energy metabolism-related genes (*TAT*, *TPI*, *HK*) were down-regulated in the combined exposure group. Pathways associated with glutathione metabolism and cytochrome P450 were notably affected, and the combined exposure suppressed the expression of immune-related genes such as *CYP450*, *GST*, and *UGT*. In summary, we found an enhanced toxicological impact of NPs when combined with Cu^{2+}. Thus, this study provides insights into the toxicological mechanisms of NPs and Cu^{2+} in aquatic organisms, highlighting their ecological risks to aquatic ecosystems.

KEYWORDS

***Eriocheir sinensis*, nanoplastics, copper, combined toxicity, transcriptome, immunity**

1 Introduction

The proliferation of plastic waste in the environment, driven by rapid industrialization and urbanization, has led to the emergence of microplastics (MPs) as ubiquitous pollutants (Shukla et al., 2022). MPs are plastic particles smaller than 5 mm in diameter (Hoseini and Bond, 2022). Previous studies have reported that MPs concentrations have reached 9,000 particles/m^3 in the northeastern Pacific Ocean and 4,137 particles/m^3 in the Yangtze River estuary (Zhao et al., 2014; Bagaev et al., 2021). Plastics smaller than 1,000 nm are classified as nanoplastics (NPs) (Tian et al., 2019). Due to their reduced size and increased surface area, NPs possess heightened abilities to penetrate biological barriers and persist in aquatic ecosystems, exacerbating their toxic effects on aquatic organisms (Turan et al., 2019; López et al., 2022). Research has demonstrated that NPs inhibit the growth of *Artemia franciscana* (Varó et al., 2019), induce neurotoxicity, and reduce survival rates in *Oryzias latipes* (Manabe et al., 2011). Furthermore, NPs disrupt glucose metabolism in zebrafish (Brun et al., 2019). NPs act as carriers for toxic substances in aquatic environments due to their large surface area and strong adsorption capacity (Shen et al., 2019; Dayal et al., 2024).

Copper (Cu) is one of the most prevalent heavy metals in aquatic ecosystems, originating from mining, industrial activities, agricultural pesticides, antifouling paints, and aquaculture practices (Chen et al., 2015). In anthropogenically impacted surface waters, Cu concentrations can reach as high as 560 μg/L (Santos et al., 2022). Cu exposure has been reported to induce various biochemical, physiological, and behavioral abnormalities in fish (Haverroth et al., 2015; Sonnack et al., 2015). Although Cu is an essential element for crustaceans, the high concentrations of copper can be potentially toxic (Zhang F. et al., 2022). The high concentrations of copper can damage the gills and hepatopancreas of *Litopenaeus vannamei* (Frías-Espericueta et al., 2008) and cause abnormal bioaccumulation in the carapace and hepatopancreas of *Scylla paramamosain* (Luo et al., 2020). Chronic Cu exposure has also been linked to oxidative stress, immune dysfunction, and hepatopancreatic damage in *Eriocheir sinensis* (Bu et al., 2022).

The Yangtze River, China's largest and the world's third-largest river, serves as a vital breeding and foraging ground for numerous fishery species along the western Pacific coastline (Zhang et al., 2023). It is also the most important spawning area for *E. sinensis*, a species of significant economic value in China (Chen and Zhang, 2007; Shen et al., 2023b). Mature crabs migrate to the estuarine waters of the Yangtze River to spawn during winter (Qin et al., 2024). The gills, as the primary organ exposed to environmental pollutants, are prone to heavy metal accumulation, leading to disrupted osmoregulation and cellular homeostasis (Lee et al., 2010; Ortega et al., 2017). Rich in innate immune cells and stress response pathways, gills play a crucial role in defending crustaceans against environmental challenges (Shen et al., 2023a). In the Yangtze River estuary, the co-occurrence of MPs, Cu, and other pollutants has been reported, posing potential risks to aquatic organisms (Liu C. et al., 2022; Yu et al., 2023). The parent crabs of *E. sinensis* may be adversely affected by NPs and Cu.

Given the common environmental entry pathways of Cu and NPs, their interaction may have synergistic toxic effects on aquatic organisms (Zhang F. et al., 2022). Therefore, understanding the combined effects of NPs and Cu on *E. sinensis* is essential to elucidate the mechanisms of their joint toxicity. This study may provide insights into the role of NPs and Cu as potential risk factors for the pollution of the spawning grounds of *E. sinensis*, to better assess their impacts on the structure and function of the ecosystem of the Yangtze River estuary.

2 Materials and methods

2.1 Chemicals and experimental animals

Copper sulfate pentahydrate ($CuSO_4{\cdot}5H_2O$, ≥99.0%) was purchased from Sinopharm Chemical Reagent Co., Ltd. (Shanghai, China). A 1 g/L copper ion stock solution was prepared using distilled water and stored in a light-proof brown bottle. Green fluorescent polystyrene nanoplastics (100 ± 0.4 nm) were obtained from the Bestar Research Center (Tianjin, China).

A total of 240 mature female *E. sinensis*, with an average body weight of 92.27 ± 10.34 g, were transported to the laboratory in November 2023. Before the experiment, the crabs were acclimated for two weeks in aquaculture tanks (200 cm × 120 cm × 50 cm) disinfected with potassium permanganate. The water temperature was maintained at 13 ± 3°C, pH at 7.0–7.5, and dissolved oxygen levels above 6 mg/L. Tap water was aerated for 24 hours to remove residual chlorine before use. During acclimation, crabs were fed daily at 18:00 with commercial feed (Changzhou Haida Biotechnology Co., Ltd., Changzhou, China) at a feeding rate of 1% of their total body weight, and uneaten food was promptly removed.

2.2 Experimental design and sampling

The concentration of microplastics in the aquatic environment of the Yangtze River estuary, an important spawning ground for *E. sinensis*, was 4.173 items/L. The test concentration of NPs was set at 0.4 mg/L (5.4 items/L) in conjunction with previous studies (Zhao et al., 2014; Liu et al., 2019; Yang et al., 2022). The Cu^{2+} concentration in the Yangtze River estuary was 0.07 mg/L, and the test concentration of Cu^{2+} was set at 0.1 mg/L in conjunction with environmentally relevant concentrations and previous studies (Yang et al., 2008; Ren et al., 2011; Zhang C. et al., 2022).

The crabs were randomly divided into four groups: a control group with no drug treatment, a group treated with 0.4 mg/L nanoplastics (NPs group), a group treated with 0.1 mg/L Cu^{2+} (Cu group), and a group treated with 0.4 mg/L nanoplastics and 0.1 mg/L Cu^{2+} (NPs + Cu group). Each group included three replicates, with 20 crabs per replicate. Oxygenation was continuous during the test period. The daily feeding rate was 1% of the crabs' total weight. The remaining feed was cleaned up in time, and the water was changed every 7 days. Referring to the studies of Yang et al. (Yang et al., 2022) and Pan et al. (Pan et al., 2023), the time of the exposure test was set to 21 days.

On day 21, nine crabs from each parallel group were randomly selected for sampling. The crabs were anesthetized on ice, and their gill tissues were immediately separated. Samples for biochemical, transcriptomic, and qRT-PCR analyses were stored at -80°C. Three crabs were randomly taken from each parallel group as biological replicates for histological experiments, and the gill tissue samples were placed in 4% paraformaldehyde and fixed at 4°C for 24 hours.

2.3 Histological analysis

Gill samples fixed in 4% paraformaldehyde were sequentially dehydrated in graded ethanol and xylene solutions. The dehydrated samples were embedded in paraffin and sectioned into 4 μm slices using a microtome. Sections were stained using the hematoxylin-eosin (H&E) method. Histopathological changes were observed and photographed using a Nikon Eclipse Ci microscope at 200× magnification.

2.4 Biochemical analysis

Approximately 0.2 g of gill tissue was homogenized in 1 mL of extraction buffer at 4°C using a homogenizer. The homogenate was centrifuged at 12,000 rpm for 10 minutes, and the supernatant was collected for biochemical assays. Commercial kits (Jiangsu AIDISEN Biotechnology Co., Ltd., Yancheng, China) were used to measure the following biochemical parameters. Antioxidant indicators: superoxide dismutase (SOD), catalase (CAT), glutathione peroxidase (GSH-Px), glutathione (GSH), malondialdehyde (MDA), and total antioxidant capacity (T-AOC). Immune indicators: acid phosphatase (ACP), alkaline phosphatase (AKP), lysozyme (LZM), metallothionein (MT), caspase-3 and caspase-9 activities.

Data were analyzed using one-way ANOVA followed by Tukey's *post hoc* test with SPSS 26 (IBM, USA). Results are expressed as mean ± standard deviation (SD), with statistical significance set at $P < 0.05$. Graphs were generated using Origin 2021.

2.5 Transcriptomic analysis

Total RNA was extracted from gill tissues using the TRIzol reagent (Aidlab, Beijing, China). RNA purity, concentration, and integrity were assessed using a NanoDrop 2000 spectrophotometer (Thermo Fisher Scientific, USA) and agarose gel electrophoresis. High-quality RNA samples were used to construct sequencing libraries, which were sequenced on the NovaSeq X Plus platform.

Raw reads underwent quality control using FastQC software. Reads containing adapters, low-quality bases (Q < 20), or an *N* content greater than 10% were removed. Clean reads were aligned to the reference genome using HISAT2 software. Differentially expressed genes (DEGs) were identified using DESeq with a threshold of adjusted $P < 0.05$ and $|\log_2(\text{fold change})| > 1$. Functional-enrichment analyses including GO and KEGG were performed to identify which DEGs were significantly enriched in GO terms and metabolic pathways at Bonferroni-corrected P-value < 0.05 compared with the whole-transcriptome background. GO functional enrichment and KEGG pathway analysis were carried out by Goatools and Python scipy software, respectively.

To validate RNA-Seq results, ten DEGs were selected for qRT-PCR analysis. These ten DEGs are *GSH-Px* (NPs vs Control), *ALF* (NPs vs NPs + Cu), *CS* (NPs vs Control), *IDH* (NPs vs Control), *ATPase* (Cu vs Control), *COX* (Cu vs Control), *GST* (NPs + Cu vs Control), *HSP60* (NPs vs NPs + Cu), *CAT* (Cu vs NPs + Cu), *ALDH* (Cu vs NPs + Cu). Gene-specific primers were designed using Primer Premier 5.0, and *β-actin* was used as the reference gene (Table 1). Each gene was tested in triplicate, and relative expression levels were calculated using the $2^{-\Delta\Delta Ct}$ method (Livak and Schmittgen, 2001).

3 Results

3.1 Morphological changes of gill tissue

Following 21-days of single and combined NPs and Cu^{2+} stresses, the histological morphology of the gill had obvious changes. The control group's gill filaments were aligned neatly, and the tissue structure of gills was complete and visible. Compared to the control group, the gill tissues in the three treatment groups exhibited varying degrees of histopathological changes. The control group exhibited significantly lower blood cell and gill septa count compared to the other three groups, along with a markedly smaller inter-septal distance. In the Cu group, a reduction in gill septa was observed, accompanied by an increased inter-septal distance, elevated blood cell counts, and slight swelling at the gill filament tips. In the NPs group, an increased number of blood cells and a widened inter-septal distance were noted, along with epithelial cell detachment. In the NPs + Cu group, a pronounced increase in blood cell accumulation, a reduction in gill septa, and an expanded inter-septal distance were observed. Additionally, significant swelling at the gill filament tips and epithelial detachment were evident (Figure 1; Table 2).

3.2 Changes in oxidative stress and immune biochemical parameters

As illustrated in Figure 2, the activities of SOD and CAT were significantly reduced in the Cu, NPs, and Cu + NPs groups compared to the control group. Notably, the Cu + NPs group showed the most pronounced reduction in SOD and CAT activity ($P < 0.05$). Additionally, the Cu + NPs group exhibited significantly elevated levels of GSH-Px, GSH, MDA, and T-AOC compared to the control group ($P < 0.05$).

As shown in Figure 3, the activities of ACP, AKP, LZM, caspase-3, caspase-9, and the levels of MT were all elevated in the three treatment groups compared to the control group. The Cu + NPs group demonstrated significantly higher immune enzyme activities compared to the control group ($P < 0.05$).

10.3389/fmars.2025.1538734

TABLE 1 Primer sequences for qRT-PCR analysis.

Gene ID	Gene name	Forward and Reverse Primer (5′-3′)	Amplicon Length
	β-actin	GGCATCCACGAGACCACTT	267
		CTCCTGCTTGCTGATCCACAT	
gene-LOC127009970	*GSH-Px*	GTTCGGCGACCGTCTTGT	284
		CAATGTCGGAGCGGGTGA	
gene-LOC126983523	*ALF*	CTATGGCACAACGACACCG	167
		TCCTCCAGCGACCCTGAT	
gene-LOC127007736	*CS*	CCACCATCTACCGCAACC	250
		GCAAGGCCATTCATACCAG	
gene-LOC126986374	*IDH*	TTCGCTCACTCGTCCTTCC	241
		AGTTCTTGCACGCCCACA	
gene-LOC127005018	*ATPase*	GTATCGTAACGGCAGCATC	102
		CTCTTGGCATCAAACAGCA	
gene-LOC126998536	*COX*	GATGAAGACTTTCCAGGTTCCC	120
		TGGACGCATTCGACGAGGC	
gene-LOC126981066	*GST*	CCAAGTATGGCAAGGATGA	132
		GGAACAATGCTGGGAACAC	
gene-LOC127006718	*HSP60*	TGAAAGGCAAGGGCAAGT	213
		GGGTGGCACAAAGAGCAT	
gene-LOC127001632	*CAT*	CCTCTTCCCTTCCTTTATC	245
		CCTGGTCGGTCTTGTAAT	
gene-LOC126981040	*ALDH*	CAACAAACAGCCCATCGC	144
		GCTTCACCAATCTGCCTCA	

3.3 Transcriptomic analysis of the *E. sinensis* gill

3.3.1 Sequencing and assembly

After filtering out low-quality sequences, a total of 182,754,782 raw reads were obtained across the control and treatment groups. The Q30 values exceeded 95.65%, and GC contents were greater than 45.85%. The GC contents for the NPs, NPs + Cu, Cu, and control groups were 46.8%, 46.63%, 48.57%, and 48.41%, respectively, with Q30 values ranging from 94.9% to 95.47% (Supplementary Table S1). A total of 109,709 transcripts were identified (Supplementary Table S2).

3.3.2 Differential gene expression analysis

A total of 3,452 differentially expressed genes (DEGs) were identified in the NPs vs Control group (1,745 up-regulated and 1,707 down-regulated genes). Similarly, 4,648 DEGs were detected in the Cu vs Control group (2,647 up-regulated and 2,001 down-regulated genes), 2,789 DEGs in the NPs + Cu vs Control group (663 up-regulated and 2,126 down-regulated genes), 3,301 DEGs in the NPs vs NPs + Cu group (2,301 up-regulated and 1,000 down-regulated genes), and 4,117 DEGs in the Cu vs NPs + Cu group (3,099 up-regulated and 1,018 down-regulated genes) (Figure 4).

Significant differences in the expression of DEGs related to antioxidant systems, immune defense, and energy metabolism were observed across the five comparison groups. *Carbonic anhydrase* (*CA*) was consistently downregulated in all five comparisons. Genes such as *ATP synthase* (*ATPase*) and *aldehyde dehydrogenase* (*ALDH*) were significantly downregulated in the NPs vs Control, Cu vs Control, and NPs + Cu vs Control groups. *Phospholipid-transporting ATPase* (*TAT*) was uniquely downregulated in the NPs + Cu vs Control group, while being upregulated in the other groups. Similarly, *Cytochrome P450* (*CYP450*) was significantly downregulated in the NPs vs Control, Cu vs Control, and NPs + Cu vs Control groups but showed upregulation in the Cu vs NPs + Cu comparison. *Glutathione S-transferase* (*GST*) was downregulated in the NPs vs Control, Cu vs Control, and NPs + Cu vs Control groups but was upregulated in the NPs vs NPs + Cu and Cu vs NPs + Cu groups. Interestingly, *UDP-glucosyltransferase* (*UGT*) was downregulated exclusively in the NPs + Cu vs Control group, while being upregulated in the other four comparisons (Table 3).

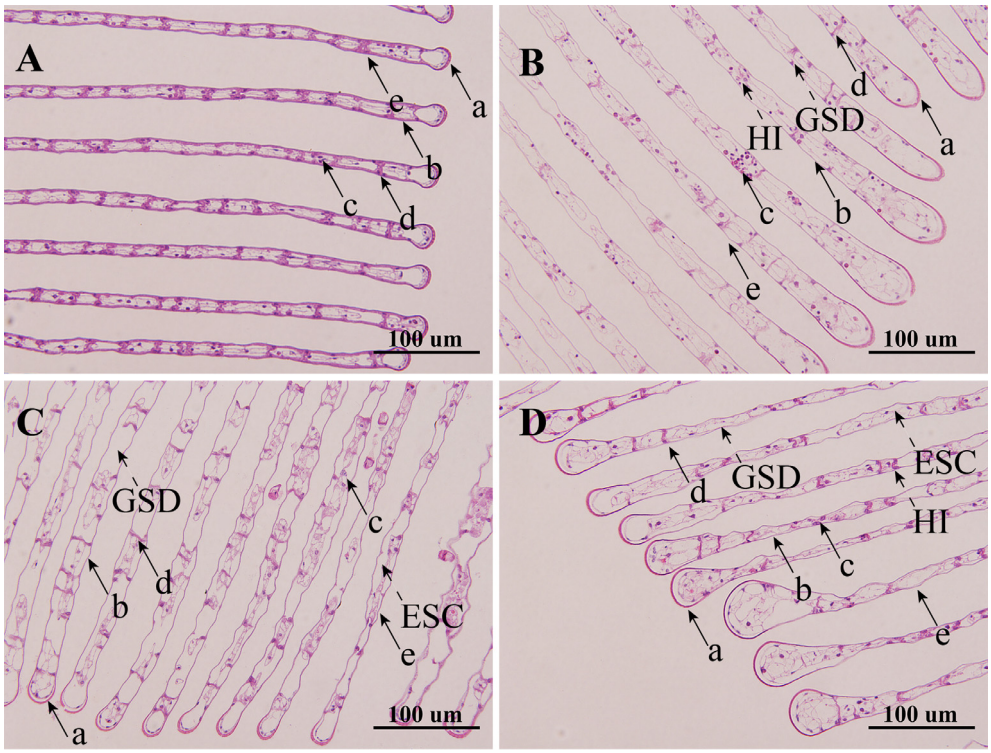

FIGURE 1
Effects of individual or combined exposure to NPs and Cu^{2+} on the morphological structure of gills of *E. sinensis*. **(A)** Control group, **(B)** Cu group, **(C)** NPs group, **(D)** NPs + Cu group. a: cuticle; b: epithelial cells; c: hemocytes; d: septum; e: gill filaments. GSD, Gill septum decrease; HI, Hemocytes increase; ECS, Epithelial cells shed.

3.3.3 GO enrichment analysis of DEGs

The GO enrichment analysis of DEGs revealed distinct functional enrichments across the comparison groups. In the NPs vs Control group, DEGs were significantly enriched in GO terms related to "organic acid catabolic process", "carboxylic acid catabolic process", and "cellular amino acid catabolic process". In the Cu vs Control group, DEGs were primarily enriched in "translation", "peptide biosynthetic process", and "amide biosynthetic process". For the NPs + Cu vs Control group, DEGs were significantly enriched in terms such as "serine-type endopeptidase inhibitor activity", "endopeptidase regulator activity", and "endopeptidase inhibitor activity". Pathways related to metabolism were significantly enriched in the NPs vs NPs + Cu and Cu vs NPs + Cu groups (Figure 5).

3.3.4 KEGG pathway enrichment analysis of DEGs

In the NPs vs Control group, 1,592 DEGs were mapped to 338 KEGG pathways, with 22 pathways significantly enriched. These pathways primarily included "Bile secretion", "Oxidative phosphorylation", and "Citrate cycle (TCA cycle)". In the Cu vs Control group, 2,307 DEGs were annotated to 342 pathways, with 18 pathways significantly enriched, such as "Ribosome, Glutathione metabolism", and "Tryptophan metabolism". For the NPs + Cu vs Control group, 1,159 DEGs were mapped to 324 pathways, with 22 pathways significantly enriched, including "Glutathione metabolism", "Metabolism of xenobiotics by cytochrome P450", and "Glycolysis / Gluconeogenesis" (Figure 6).

Genes involved in energy metabolism exhibited distinct expression patterns across groups. *Triosephosphate isomerase* (*TPI*)

TABLE 2 Gill tissue gill lobe parameters of different treatments.

Index	Control group	Cu group	NPs group	NPs + Cu group
Number of blood cells	25 ± 2.65^{a}	43.33 ± 5.77^{c}	35.67 ± 3.21^{b}	41.00 ± 1.00^{bc}
Number of septum	14.33 ± 1.15^{a}	8.67 ± 0.57^{b}	7.33 ± 0.57^{bc}	6.67 ± 0.57^{d}
Septum distance (um)	51.50 ± 7.92^{a}	128.17 ± 46.31^{b}	114.83 ± 34.94^{b}	158.50 ± 61.15^{b}

Data are presented as mean ± standard deviation (n=3). Different letters indicate significant differences between treatment groups ($P < 0.05$).

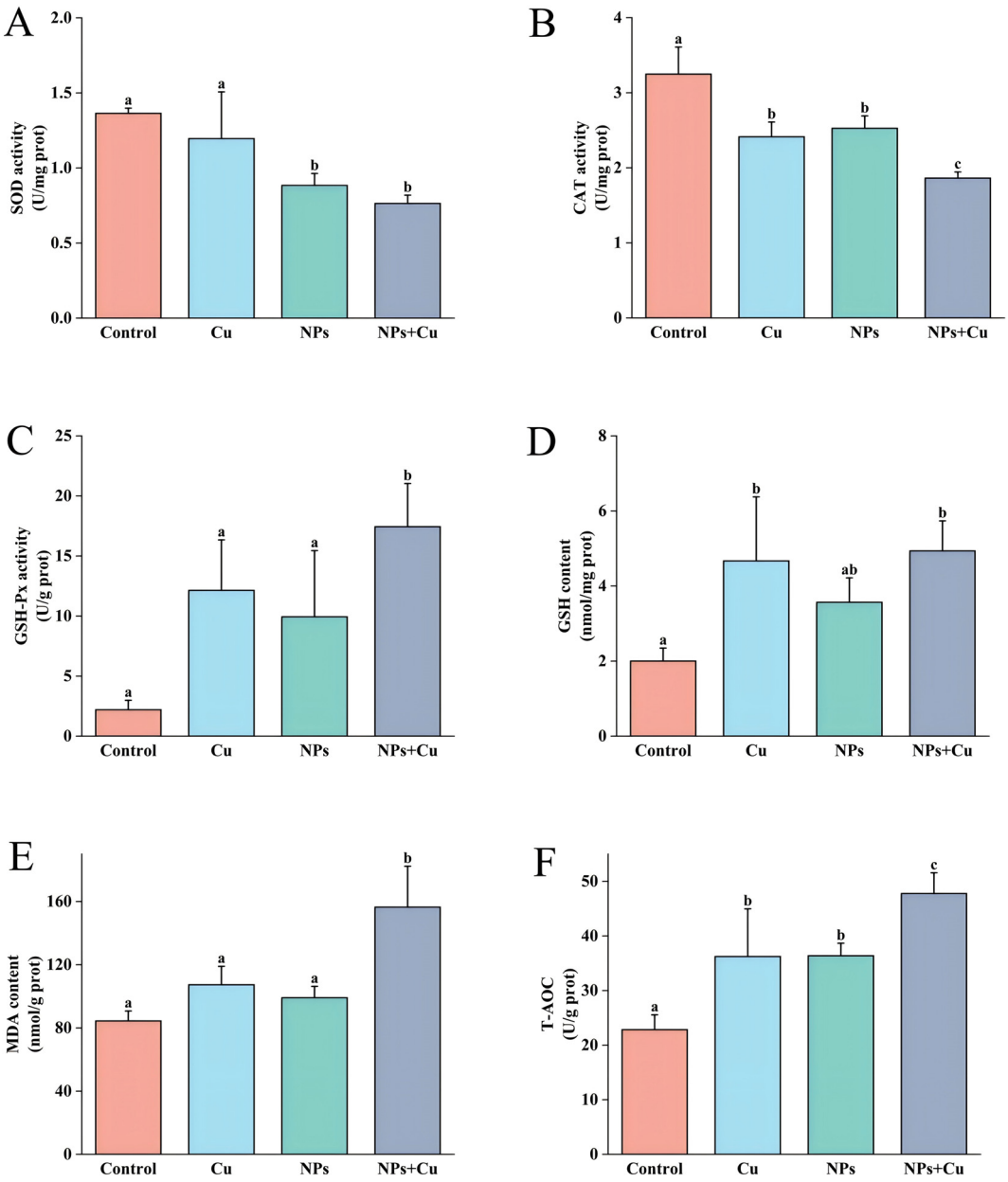

FIGURE 2
Effects of individual and combined exposure to NPs and Cu^{2+} on antioxidant parameters in the gills of *E. sinensis*. Levels of SOD **(A)**, CAT **(B)**, GSH-Px **(C)**, GSH **(D)**, MDA **(E)**, and T-AOC **(F)** were measured in all groups on day 21 of exposure. Data are presented as mean ± standard deviation (n=3). Different letters indicate significant differences between treatment groups ($P < 0.05$).

was significantly upregulated in the NPs vs Control, NPs + Cu vs Control, and NPs vs NPs + Cu groups. *Hexokinase* (*HK*) was upregulated in the NPs vs Control and NPs vs NPs + Cu groups but downregulated in the NPs + Cu vs Control group.

3.3.5 Validation of RNA-seq with qRT-PCR

To verify the reliability of the transcriptomic data, ten DEGs were selected from the transcriptome database for validation using qRT-PCR. These ten DEGs are *GSH-Px* (NPs vs Control), *ALF* (NPs vs NPs + Cu), *CS* (NPs vs Control), *IDH* (NPs vs Control), *ATPase* (Cu vs Control), *COX* (Cu vs Control), *GST* (NPs + Cu vs Control), *HSP60* (NPs vs NPs + Cu), *CAT* (Cu vs NPs + Cu), *ALDH* (Cu vs NPs + Cu). The expression patterns of these genes were consistent with the transcriptomic results, confirming the robustness and reliability of the sequencing data (Figure 7).

4 Discussion

4.1 Histopathological damage induced by NPs and Cu^{2+}

Gill histological analysis has been widely utilized as a practical tool to assess environmental stress in aquaculture, particularly in *E. sinensis* (Yang et al., 2021; Wang et al., 2023). Under Cu^{2+} stress, the

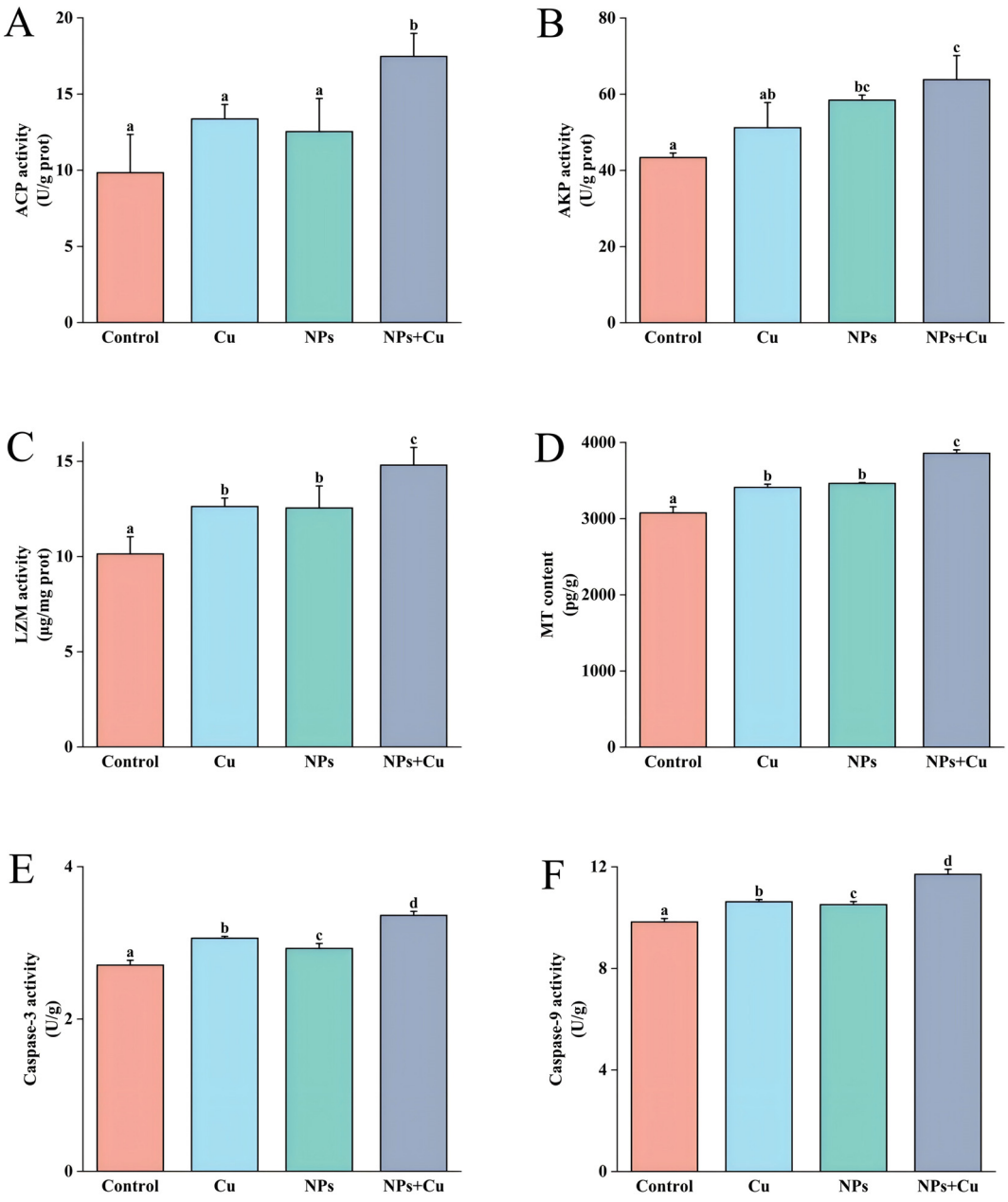

FIGURE 3
Effects of individual and combined exposure to NPs and Cu^{2+} on immune parameters in the gills of *E. sinensis*. Levels of ACP **(A)**, AKP **(B)**, LZM **(C)**, MT **(D)**, caspase-3 **(E)**, and caspase-9 **(F)** were measured in all groups on day 21 of exposure. Data are presented as mean ± standard deviation (n=3). Different letters indicate significant differences between treatment groups ($P < 0.05$).

gill cell membranes of *E. sinensis* exhibited extensive diffusion and fragmentation, with nuclei showing signs of disintegration (Tang et al., 2021). At pH 7.8, cadmium (Cd) stress in *E. sinensis* led to an abnormal increase in hemocytes within gill hemolymphatic sinuses (Zhao et al., 2021). Similarly, NPs have been found to accumulate in the gills of *Corbicula fluminea*, exacerbating biotoxicity (Li et al., 2020). In the present study, gill damage was more severe in the combined exposure group (NPs + Cu) than in the NPs or Cu^{2+} groups alone. In the NPs + Cu group, significant swelling at the gill tips, the number of blood cells in the gill lobes was increased, and epithelial shedding were observed. This may be due to the ability of NPs to act as carriers, facilitating the transport of other pollutants into organisms, and thereby increasing bioaccumulation (Zarfl and Matthies, 2010). Previous studies have demonstrated that NPs can adsorb heavy metals and enhance their toxicity in aquatic organisms (Zhu et al., 2024). As gills are the primary organs directly exposed to the aquatic environment, they exhibit more pronounced damage under stress (Silvestre et al., 2005). Xing et al (Xing et al., 2025). reported that combined stress can aggravate nitrite or sulfide-induced damage to the gill tissues of *E. sinensis*. This study suggested that the combined stress might exacerbate the stress of NPs or Cu^{2+} on *E. sinensis*.

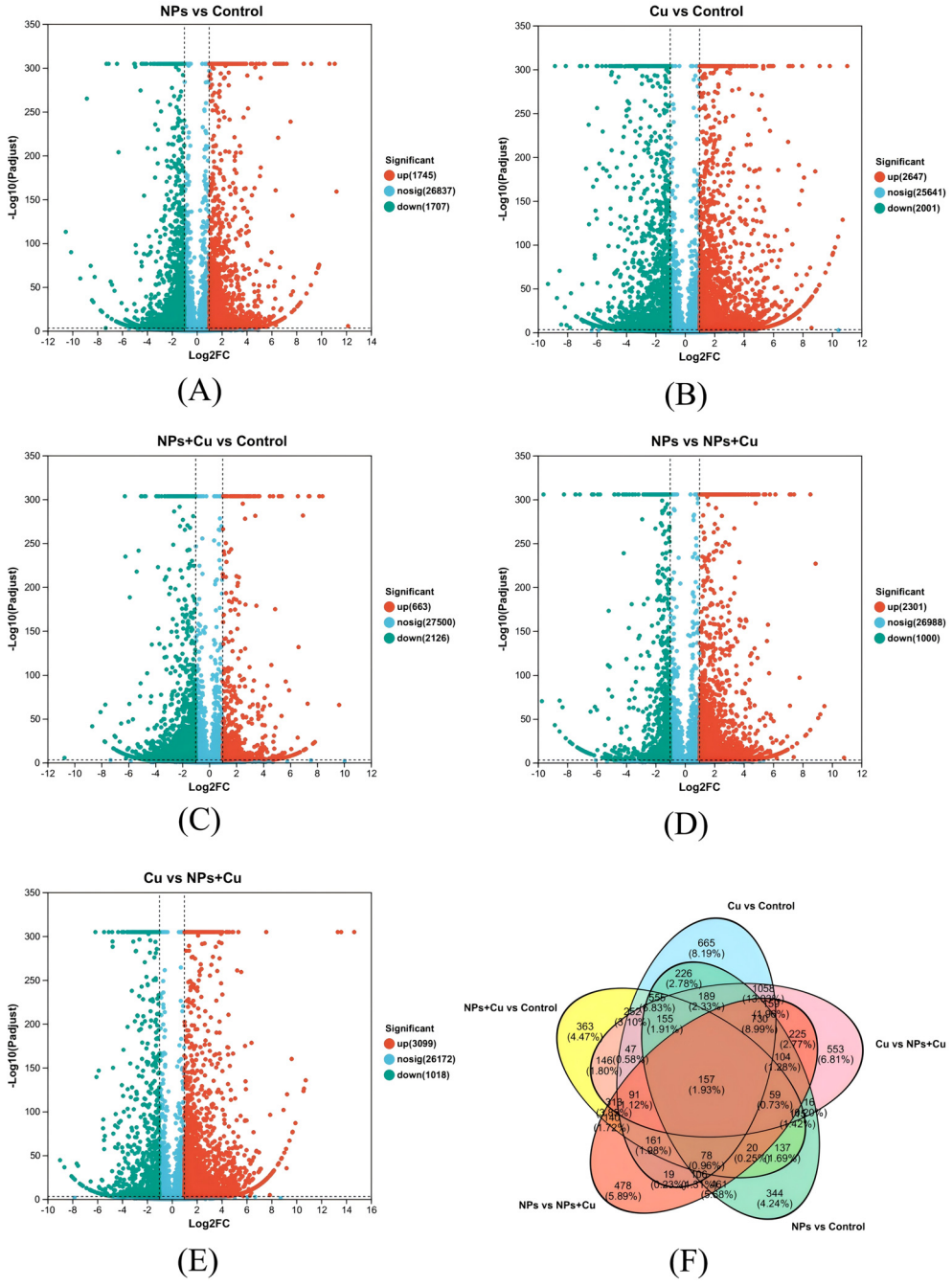

FIGURE 4
Analysis of differentially expressed genes **(A–E)** Volcano map of DEGs; **(F)** Venn diagram of DEGs.

4.2 Effects of NPs and Cu^{2+} exposure on enzyme activities

NPs and Cu^{2+} are known to accumulate in the tissues of crustaceans, leading to oxidative damage, apoptosis, autophagy, and immune responses (Feng et al., 2022; Li et al., 2024). The antioxidant system serves as a non-specific adaptive mechanism in crustaceans to counteract oxidative damage by eliminating excess reactive oxygen species (ROS) via a series of antioxidant enzymes, including SOD, CAT, GSH, and GSH-Px (Valencia-Castañeda et al., 2020; Frías-Espericueta et al., 2022). SOD catalyzes the conversion of O_2^- and H^+ to H_2O_2, and then CAT and GSH-Px can further convert H_2O_2 to non-toxic H_2O. Therefore, SOD-CAT and SOD-GSH-Px are considered to be the first important antioxidant line of defense (Zeng et al., 2016). In this study, the NPs + Cu group had the lowest activity of SOD, CAT, and but the highest activity of GSH-Px indicating the activation of the antioxidant system (Hu and Palić, 2020). GSH is the most abundant cytoplasmic scavenger that neutralizes ROS and acts as a second line of defense (Lu et al., 2018). GSH can bind to metals to

10.3389/fmars.2025.1538734

TABLE 3 DEGs potentially associated with antioxidant system, immune defense, and energy metabolism.

Functional Group/Gene	Description	Regulation	NPs vs Control	Cu vs Control	NPs+Cu vs Control	NPs vs NPs+Cu	Cu vs NPs+Cu
Antioxidant system							
SOD	superoxide dismutase	Up	X	X		X	X
		Down			X		
CAT	catalase	Down		X			X
GST	glutathione S-transferase	Up				X	X
		Down	X	X	X		
GSH	glutathione	Up		X	X		X
GSS	glutathione synthetase	Down		X			X
GSH-Px	glutathione peroxidase	Up	X	X			X
PRDX	peroxiredoxin	Up				X	X
		Down	X	X	X		
Immune defense							
HSP60	heat shock 90	Down				X	
HSP70	heat shock 70	Up	X	X	X	X	X
TRIM	tripartite motif containing protein	Up		X	X		X
		Down	X			X	
TLR	toll-like receptor	Up					X
		Down	X	X	X		
MRC1	macrophage mannose receptor 1	Up		X	X		
		Down				X	X
FREP1	fibrinogen C domain-containing protein 1	Up				X	
		Down	X	X	X		X
LZM	lysozyme	Up	X	X	X		X
		Down				X	
CLEC	C-type lectin	Up		X	X		
		Down	X			X	
C1	complement component receptor 1	Up	X	X	X	X	X
C2	complement C2	Up	X	X		X	X
		Down			X		
KLRG2	killer cell lectin-like receptor subfamily G member 2	Up	X	X		X	X
EGR	early growth response protein	Up		X		X	X
		Down			X		
CASP1	caspase-1	Up	X	X	X	X	X
CASP2	caspase-2	Down		X	X	X	X
CASP8	caspase-8	Up	X		X		
CYP450	cytochrome P450	Up				X	

(Continued)

TABLE 3 Continued

Functional Group/Gene	Description	Regulation	NPs vs Control	Cu vs Control	NPs+Cu vs Control	NPs vs NPs+Cu	Cu vs NPs+Cu
Immune defense							
		Down	X	X	X		X
UGT	UDP-glucosyltransferase	Up	X	X		X	X
		Down			X		
IL-1	interleukin-1	Up				X	
		Down		X			
IL-3	interleukin-3	Up				X	X
ALF	anti-lipopolysaccharide factor	Up	X	X	X	X	
		Down					X
Energy metabolism							
ATPase	ATP synthase	Up					X
		Down	X	X	X	X	
TAT	phospholipid-transporting ATPase	Up	X	X		X	X
		Down			X		
ABC	ATP-binding cassette	Up	X	X		X	X
		Down			X		
ALDH	aldehyde dehydrogenase	Down	X	X	X	X	X
COX	cytochrome c oxidase subunit	Down	X	X		X	X
CA	carbonic anhydrase	Down	X	X	X	X	X
NOX	NADPH oxidase	Up	X	X		X	
Orct	organic cation transporter	Up		X		X	X
		Down	X		X		
SLC22A	solute carrier family 22 member 20	Up					X
		Down	X	X	X	X	
SDH	Succinate dehydrogenase	Down	X	X		X	X
IDH	isocitrate dehydrogenase	Down	X	X		X	X
CS	citrate synthase	Down	X			X	
ND	NADH dehydrogenase	Down					X

"X" represents that the gene is differentially expressed in this comparison group.

eliminate their toxic effects, and elevated GSH levels appear to be an antioxidant adaptation to chronic exposure (Kanak et al., 2014). The elevated GSH content in the Cu group and the NPs + Cu group suggests that the toxic effects of metals are being mitigated. Excessive ROS reacts with phospholipids and enzymes on biological membranes, forming lipid peroxidation products such as MDA, which is commonly used to measure oxidative damage (Liu et al., 2008). Increased MDA content and T-AOC activity in the exposure groups indicate oxidative damage and enhanced antioxidant capacity in response to adverse environmental conditions (Wei et al., 2023). Similarly, co-exposure to Cd and MPs has been shown to exacerbate oxidative damage in zebrafish (Lu et al., 2018). Notably, MDA content and T-AOC activity were highest in the combined exposure group, suggesting greater oxidative stress.

ACP and AKP are key components of lysosomes, while LZM forms part of the hydrolytic enzyme system, playing a critical role in non-specific immunity in crustaceans (Chen et al., 2017; Bao et al., 2020). Pre-caspase-3 is distributed in the cytoplasm and mitochondria, where it can be activated by upstream caspase-8 and caspase-9 in signal transduction pathways (Liu et al., 2011). Caspase-3, an effector caspase, is pivotal in the cascade of apoptotic reactions (Nicholson, 1999), and its role in Cd-induced apoptosis has been well established (Cheng et al., 2021).

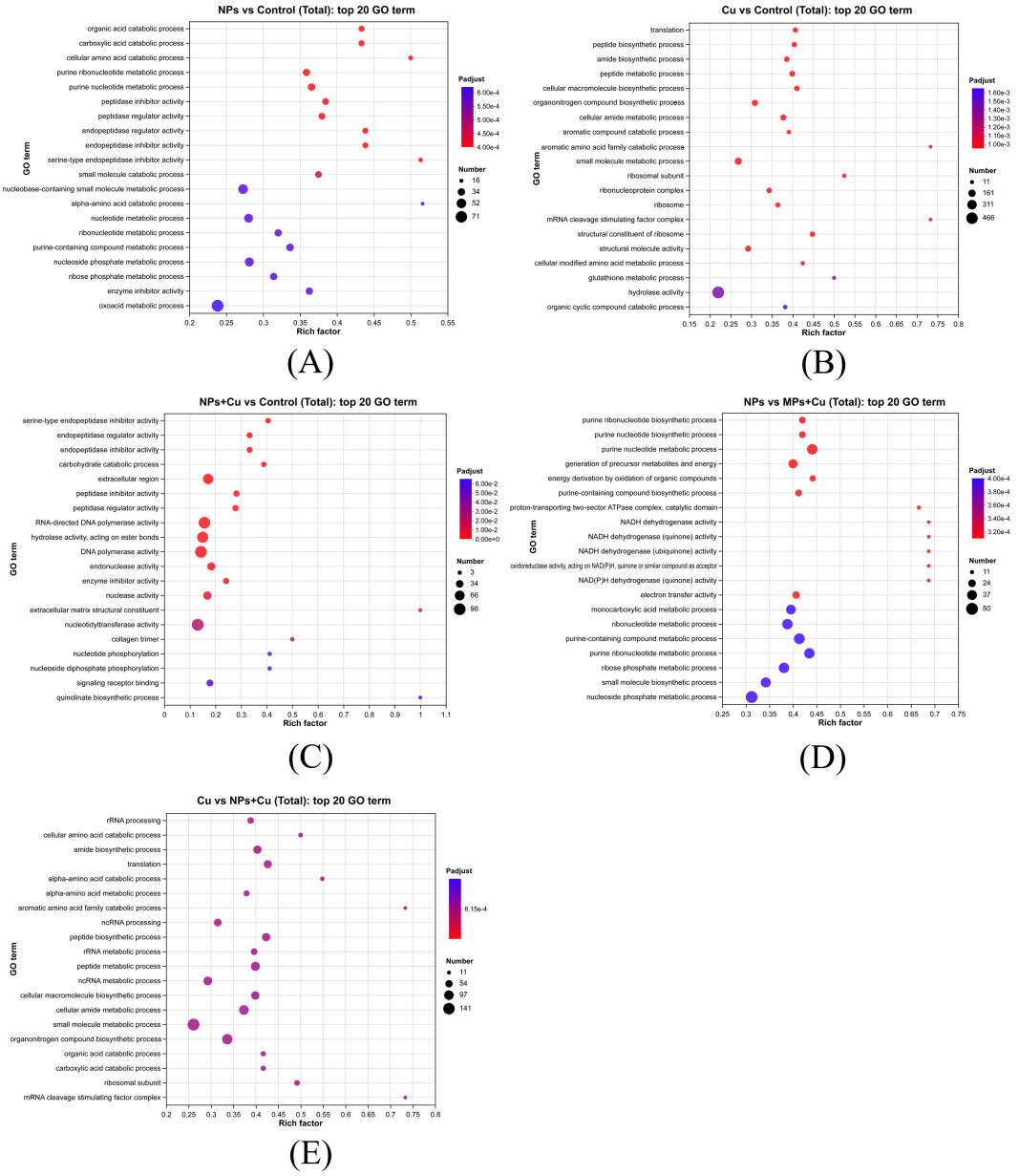

FIGURE 5
Bubble diagram of top 20 GO terms enriched by DEGs **(A–E)**.

In the present study, caspase-3 and caspase-9 were significantly higher in the treated group than in the control group, and the highest activity was observed in the combined exposure group. It was hypothesized that NPs and Cu2+ exposure induced excessive ROS production and led to lipid peroxidation, increasing the activities of apoptosis-related enzymes caspase-3 and caspase-9 in gill tissues (Cheng et al., 2020). MTs, a class of metal-inducible proteins, are easily induced by metals and can indirectly reflect the level of heavy metal pollution in the environment (Amiard et al., 2006). In this study, immune enzyme activities in the NPs + Cu group were higher than in other groups and significantly higher than in the control group. Consistent with our findings, co-exposure to Cd and MPs has been reported to enhance metal toxicity in zebrafish (Lu et al., 2018). Compared to single exposures, combined exposure increased gill toxicity, likely due to the accumulation of NPs and Cu^{2+} on the gills, which inhibited aerobic metabolic activities (Pacheco et al., 2018). Additionally, the presence of polystyrene nanoparticles may exacerbate the toxicity of metal ions (Lee et al., 2019).

4.3 Effects of NPs and Cu^{2+} exposure on energy metabolism

The gills, as the primary organ directly exposed to the aquatic environment, play a crucial role in osmoregulation (Dolomatov et al., 2012). Genes associated with osmoregulation, such as *carbonic anhydrase* (*CA*), were significantly downregulated across all five

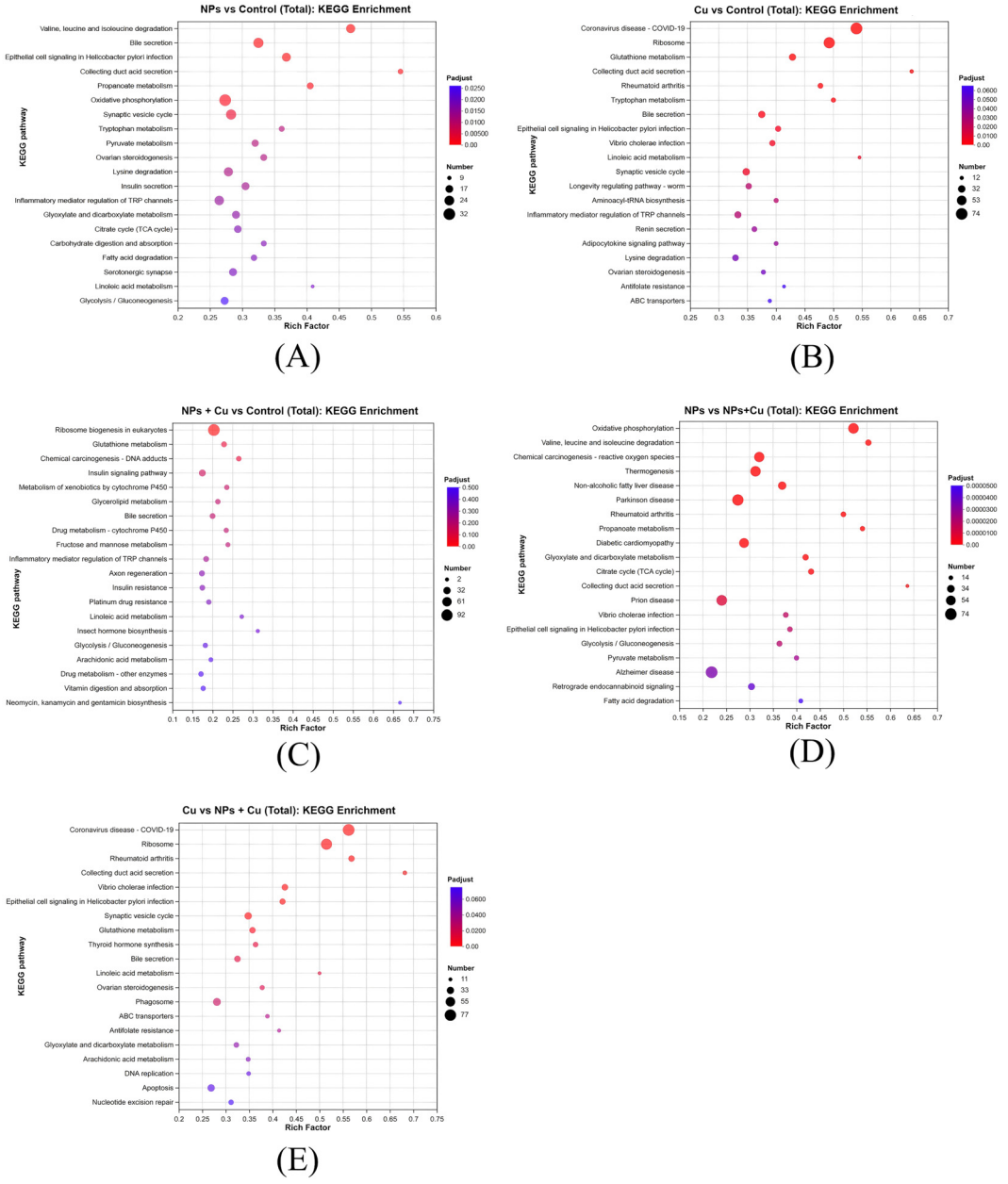

FIGURE 6
Bubble diagram of KEGG pathways enrichment by DEGs **(A–E)**.

comparison groups (Hui et al., 2014). Osmoregulation is an energy-intensive process, and pathways related to energy metabolism were markedly affected in both single and combined exposure groups (Chong-Robles et al., 2014). Genes related to energy metabolisms, such as *ATP synthase* (*ATPase*) and *aldehyde dehydrogenase* (*ALDH*), were significantly downregulated in the NPs vs Control, Cu vs Control, and NPs + Cu vs Control groups. Conversely, *phospholipid-transporting ATPase* (*TAT*) was significantly downregulated only in the NPs + Cu vs Control group. *TAT* gene expression in *Litopenaeus vannamei* was markedly suppressed under stress conditions (Zhang et al., 2018). It is hypothesized that combined exposure will have the greatest effect on *TAT* gene expression, affecting cellular phospholipid transport and hence energy metabolism in *E. sinensis*.

Organisms rely on gluconeogenesis to synthesize glucose and sustain their energy requirements (Cota-Ruiz et al., 2015). KEGG pathway analysis revealed significant enrichment of the glycolysis/gluconeogenesis pathway in the NPs vs Control and NPs + Cu vs Control groups. Triosephosphate isomerase (TPI), a critical glycolytic enzyme that catalyzes the conversion of dihydroxyacetone phosphate (DHAP) to glyceraldehyde 3-phosphate (GAP). GAP is an intermediate product of glycolysis, and differential expression of the *TPI* gene may affect GAP production and thus glycolysis (Liu P. et al., 2022).

Hexokinase (*HK*) expression was significantly upregulated in the NPs vs Control and NPs vs NPs + Cu groups but notably downregulated in the NPs + Cu vs Control group. As a pivotal regulator in the glycolysis pathway, HK catalyzes the initial step of

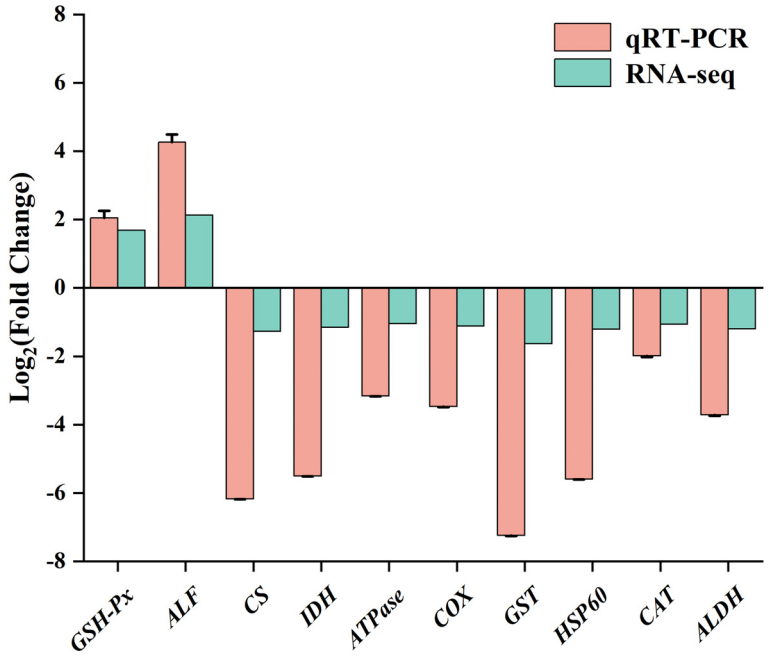

FIGURE 7
Validation of RNA sequences by qRT-PCR.

glycolysis, converting glucose into glucose-6-phosphate (Enes et al., 2009; Jia et al., 2020). Glucose-6-phosphate may be involved in other metabolic pathways such as gluconeogenesis and the pentose-phosphate pathway (Enes et al., 2009). Inhibition of key glycolytic enzymes promotes gluconeogenesis (Ding et al., 2020). Combined exposure to NPs and Cu^{2+} led to a significant reduction in *HK* expression compared to single-stressor exposures, disrupting glycolysis and gluconeogenesis pathways. This impairment in energy metabolism contributed to gill damage. GO analysis further revealed significant enrichment of metabolism-related pathways in the NPs vs NPs + Cu and Cu vs NPs + Cu groups. Similarly, Ding et al. (Ding et al., 2020). reported that *Larimichthys crocea* mitigates toxicity by modulating glycolysis and gluconeogenesis under stress conditions. NPs affected the energy metabolism of *E. sinensis*, and combined exposure results in enhanced toxicity to the energy metabolism system.

4.4 Effects of NPs and Cu^{2+} exposure on immune regulation mechanisms

KEGG enrichment analysis revealed significant involvement of pathways such as glutathione metabolism, xenobiotic metabolism by cytochrome P450, and drug metabolism-cytochrome P450 in the NPs + Cu vs Control group. Pathways related to glutathione metabolism were significantly enriched in the Cu vs Control, NPs + Cu vs Control, and Cu vs NPs + Cu groups. The ability of organisms to resist environmental stress largely depends on the metabolism and detoxification of xenobiotics, a process typically divided into two stages (Esteves et al., 2021). *CYP450* expression was significantly downregulated in NPs vs Control, Cu vs Control, and NPs + Cu vs Control, but upregulated in Cu vs NPs + Cu. CYP450 enzymes are critical for the initial phase of the three-stage detoxification process, where toxins are transformed into intermediate metabolites (Awali et al., 2019). Compared to the Cu group, co-exposure further inhibited *CYP450* gene expression, potentially hindering the conversion of toxins into intermediate metabolites. CYP450 is classified as a Phase I biotransformation enzyme, whereas GST and UGT are Phase II detoxification enzymes (Debersac et al., 2001). GST and UGT catalyze the conjugation of peroxidative products and electrophiles with glutathione (GSH) and glucuronic acid (GA) respectively, resulting in more polar derivatives that are more easily excreted (Rodrigues et al., 2018).

The inhibition of Phase I detoxification processes by co-exposure to NPs and Cu^{2+} likely impairs Phase II detoxification as well. This observation is supported by differential gene expression analysis, which showed that *GST* was significantly downregulated in NPs vs Control, Cu vs Control, and NPs + Cu vs Control, but upregulated in NPs vs NPs + Cu and Cu vs NPs + Cu. *UGT* expression was significantly downregulated only in NPs + Cu vs Control, while it was upregulated in the other four comparisons. Previous studies have demonstrated that exposure to imidacloprid can cause potential genotoxic effects in *E. sinensis*, inhibit *GST* transcription, and partially suppress Phase II detoxification processes (Hong et al., 2020). In *Litopenaeus vannamei*, salinity stress induces *UGT* gene enrichment across multiple pathways, particularly those involved in immune responses (Farhadi et al., 2022). Studies on *Caenorhabditis elegans* (Zhu et al., 2024), *Tachypleus tridentatus* (Arif et al., 2022), *Artemia salina* (Ahmadzadeh et al., 2025), and *Raphidocelis subcapitata* (Bellingeri et al., 2019) have similarly reported that co-exposure to NPs and Cu^{2+} enhanced toxicity to the immune system compared to single-stressor exposure. Similarly, the current study shows that co-exposure to NPs and Cu^{2+} suppressed the expression of

immune-related genes, thereby impairing immune system functionality compared to single-stressor exposure groups.

5 Conclusion

Given the ubiquitous presence of NPs and Cu^{2+} in aquatic environments, *E. sinensis* is likely to face prolonged co-exposure to these pollutants. This study demonstrates that exposure to nanoplastics (NPs) and copper ions (Cu^{2+}) disrupts the structural integrity of the gills in *E. sinensis*, impairing their metabolic and detoxification functions. Transcriptomic analysis revealed that NPs exert a more pronounced impact on metabolic pathways, while Cu^{2+} primarily affects immune system functionality under the respective stress conditions. Co-exposure to NPs and Cu^{2+} resulted in the suppression of key genes such as *TPI*, *HK*, *CYP450*, *GST*, and *UGT*, which enhances the toxic effects on metabolism and immune system. This study serves as a reference for future research on the resistance of *E. sinensis* to NPs and Cu^{2+}. It provides a new perspective for further studies on the toxic effects of crustaceans in aquatic environments.

Data availability statement

The datasets presented in this study can be found in online repositories. The names of the repository/repositories and accession number(s) can be found below. The transcriptome data are available in the NCBI SRA (accession number: PRJNA1191814).

Ethics statement

The animal study was approved by East China Sea Fisheries Research institute, Chinese Academy of Fishery Sciences. The study was conducted in accordance with the local legislation and institutional requirements.

Author contributions

JX: Conceptualization, Data curation, Formal analysis, Investigation, Methodology, Software, Validation, Visualization, Writing – original draft. GF: Funding acquisition, Resources, Supervision, Writing – review & editing. YY: Conceptualization, Supervision, Writing – review & editing.

Funding

The author(s) declare financial support was received for the research, authorship, and/or publication of this article. This research was supported by the Implementation Project for Predicting Changes in Trends of Important Species, including the Chinese Mitten Crab, in the Eastern Waters of the South Branch of the Yangtze River Estuary (11N42500663520242801).

Conflict of interest

The authors declare that the research was conducted in the absence of any commercial or financial relationships that could be construed as a potential conflict of interest.

Generative AI statement

The author(s) declare that no Generative AI was used in the creation of this manuscript.

Publisher's note

Supplementary material

The Supplementary Material for this article can be found online at: https://www.frontiersin.org/articles/10.3389/fmars.2025.1538734/full#supplementary-material

References

Ahmadzadeh, P., Naeemi, A. S., and Mansouri, B. (2025). Toxicity of polystyrene nanoplastic and copper oxide nanoparticle in artemia salina: single and combined effects on stress responses. *Mar. Environ. Res.* 203, 106831. doi: 10.1016/j.marenvres.2024.106831

Amiard, J., Amiardtriquet, C., Barka, S., Pellerin, J., and Rainbow, P. (2006). Metallothioneins in aquatic invertebrates: their role in metal detoxification and their use as biomarkers. *Aquat Toxicol.* 76, 160–202. doi: 10.1016/j.aquatox.2005.08.015

Arif, I., Shang, Y., Zhang, C., Khan, F. U., Tan, K. A., Waiho, K., et al. (2022). Combined effects of nanoplastics and heavy metal on antioxidant parameters of juvenile tri-spine horseshoe crabs. *Front. Mar. Sci.* 9. doi: 10.3389/fmars.2022.1005820

Awali, S., Abdulelah, S. A., Crile, K. G., Yacoo, K. E., Almouseli, A., Torres, V. C., et al. (2019). Cytochrome p450 and glutathione-s-transferase activity are altered following environmentally relevant atrazine exposures in crayfish (*Faxoniusvirilis*). *Bull. Environ. Contam Toxicol.* 103, 579–584. doi: 10.1007/s00128-019-02674-2

Bagaev, A., Esiukova, E., Litvinyuk, D., Chubarenko, I., Veerasingam, S., Venkatachalapathy, R., et al. (2021). Investigations of plastic contamination of seawater, marine and coastal sediments in the Russian seas: a review. *Environ. Sci. pollut. Res.* 28, 32264–32281. doi: 10.1007/s11356-021-14183-z

Bao, J., Li, X., Xing, Y., Feng, C., and Jiang, H. (2020). Effects of hypoxia on immune responses and carbohydrate metabolism in the chinese mitten crab, *Eriocheir sinensis*. *Aquac Res.* 51, 2735–2744. doi: 10.1111/are.14612

Bellingeri, A., Bergami, E., Grassi, G., Faleri, C., Redondo-Hasselerharm, P., Koelmans, A. A., et al. (2019). Combined effects of nanoplastics and copper on the freshwater alga *Raphidocelis subcapitata*. *Aquat Toxicol.* 210, 179–187. doi: 10.1016/j.aquatox.2019.02.022

Brun, N. R., van Hage, P., Hunting, E. R., Haramis, A. G., Vink, S. C., Vijver, M. G., et al. (2019). Polystyrene nanoplastics disrupt glucose metabolism and cortisol levels

with a possible link to behavioural changes in *Larval zebrafish*. *Commun. Biol.* 2, 382. doi: 10.1038/s42003-019-0629-6

Bu, X., Song, Y., Pan, J., Wang, X., Qin, C., Jia, Y., et al. (2022). Toxicity of chronic copper exposure on chinese mitten crab (*Eriocheir sinensis*) and mitigation of its adverse impact by myo-inositol. *Aquaculture* 547, 737511. doi: 10.1016/j.aquaculture.2021.737511

Chen, D., and Zhang, M. (2007). Non-volatile taste active compounds in the meat of chinese mitten crab (*Eriocheir sinensis*). *Food Chem.* 104, 1200–1205. doi: 10.1016/j.foodchem.2007.01.042

Chen, W., Ju, Y., Lin, C., Tsai, J., Chen, S., and Liao, C. (2015). Environmental stochasticity promotes copper bioaccumulation and bioenergetic response in tilapia. *Stoch Environ. Res. Risk Assess* 29, 1545–1555. doi: 10.1007/s00477-014-0993-1

Chen, Y., Huang, X., Wang, J., and Li, C. (2017). Effect of pure microcystin-LR on activity and transcript level of immune-related enzymes in the white shrimp (*Litopenaeus vannamei*). *Ecotoxicology*. 26, 702–710. doi: 10.1007/s10646-017-1802-7

Cheng, C., Ma, H., Deng, Y., Feng, J., Jie, Y., and Guo, Z. (2021). Oxidative stress, cell cycle arrest, DNA damage and apoptosis in the mud crab (*Scylla paramamosain*) induced by cadmium exposure. *Chemosphere* 263, 128277. doi: 10.1016/j.chemosphere.2020.128277

Cheng, C., Su, Y., Ma, H., Deng, Y., Feng, J., Chen, X., et al. (2020). Effect of nitrite exposure on oxidative stress, DNA damage and apoptosis in mud crab (*Scylla paramamosain*). *Chemosphere* 239, 124668. doi: 10.1016/j.chemosphere.2019.124668

Chong-Robles, J., Charmantier, G., Boulo, V., Lizárraga-Valdéz, J., Enríquez-Paredes, L. M., and Giffard-Mena, I. (2014). Osmoregulation pattern and salinity tolerance of the white shrimp *Litopenaeus vannamei* (boone 1931) during post-embryonic development. *Aquaculture* 422-423, 261–267. doi: 10.1016/j.aquaculture.2013.11.034

Cota-Ruiz, K., Peregrino-Uriarte, A. B., Felix-Portillo, M., Martínez-Quintana, J. A., and Yepiz-Plascencia, G. (2015). Expression of fructose 1,6-bisphosphatase and phosphofructokinase is induced in hepatopancreas of the white shrimp *Litopenaeus vannamei* by hypoxia. *Mar. Environ. Res.* 106, 1–9. doi: 10.1016/j.marenvres.2015.02.003

Dayal, L., Raj, D., Kumari, P., and Sinha, S. (2024). Abundance of microplastics in marine and freshwater ecosystem and it's impact on biotic and abiotic components. *Water Air Soil Pollut.* 235 (6), 1–18. doi: 10.1007/s11270-024-07199-x

Debersac, P., Heydel, J. M., Amiot, M. J., Goudonnet, H., Artur, Y., Suschetet, M., et al. (2001). Induction of cytochrome p450 and/or detoxication enzymes by various extracts of rosemary: description of specific patterns. *Food. Chem. Toxicol.* 39, 907–918. doi: 10.1016/S0278-6915(01)00034-5

Ding, J., Liu, C., Luo, S., Zhang, Y., Gao, X., Wu, X., et al. (2020). Transcriptome and physiology analysis identify key metabolic changes in the liver of the large yellow croaker (*Larimichthys crocea*) in response to acute hypoxia. *Ecotoxicol Environ. Saf* 189, 109957. doi: 10.1016/j.ecoenv.2019.109957

Dolomatov, S. I., Zukow, W., Novikov, N. Y., Muszkieta, R., Bulatowicz, I., Dzierzanowski, M., et al. (2012). The regulation of osmotic and ionic balance in fish reproduction and in the early stages of ontogeny. *Russ. J. Mar. Biol.* 38, 365–374. doi: 10.1134/S1063074012050057

Enes, P., Panserat, S., Kaushik, S., and Oliva-Teles, A. (2009). Nutritional regulation of hepatic glucose metabolism in fish. *Fish Physiol. Biochem.* 35, 519–539. doi: 10.1007/s10695-008-9259-5

Esteves, F., Rueff, J., and Kranendonk, M. (2021). The central role of cytochrome p450 in xenobiotic metabolism—a brief review on a fascinating enzyme family. *J. Xenobiotics* 11, 94–114. doi: 10.3390/jox11030007

Farhadi, A., Liu, Y., Xu, C., Han, T., Wang, X., and Li, E. (2022). Evidence from transcriptome analysis unravelled the roles of eyestalk in salinity adaptation in pacific white shrimp (*litopenaeus vannamei*). *Gen. Comp. Endocrinol.* 329, 114120. doi: 10.1016/j.ygcen.2022.114120

Feng, W., Su, S., Song, C., Yu, F., Zhou, J., Li, J., et al. (2022). Effects of copper exposure on oxidative stress, apoptosis, endoplasmic reticulum stress, autophagy and immune response in different tissues of chinese mitten crab (*Eriocheir sinensis*). *Antioxidants* 11, 2029. doi: 10.3390/antiox11102029

Frías-Espericueta, M. G., Bautista-Covarrubias, J. C., Osuna-Martínez, C. C., Delgado-Alvarez, C., Bojórquez, C., Aguilar-Juárez, M., et al. (2022). Metals and oxidative stress in aquatic decapod crustaceans: a review with special reference to shrimp and crabs. *Aquat Toxicol.* 242, 106024. doi: 10.1016/j.aquatox.2021.106024

Frías-Espericueta, M. G., Castro-Longoria, R., Barrón-Gallardo, G. J., Osuna-López, J. I., Abad-Rosales, S. M., Páez-Osuna, F., et al. (2008). Histological changes and survival of *Litopenaeus vannamei* juveniles with different copper concentrations. *Aquaculture* 278, 97–100. doi: 10.1016/j.aquaculture.2008.03.008

Haverroth, G. M. B., Welang, C., Mocelin, R. N., Postay, D., Bertoncello, K. T., Franscescon, F., et al. (2015). Copper acutely impairs behavioral function and muscle acetylcholinesterase activity in zebrafish (*Danio rerio*). *Ecotoxicol Environ. Saf* 122, 440–447. doi: 10.1016/j.ecoenv.2015.09.012

Hong, Y., Huang, Y., Wu, S., Yang, X., Dong, Y., Xu, D., et al. (2020). Effects of imidacloprid on the oxidative stress, detoxification and gut microbiota of chinese mitten crab, *Eriocheir sinensis*. *Sci. Total Environ.* 729, 138276. doi: 10.1016/j.scitotenv.2020.138276

Hoseini, M., and Bond, T. (2022). Predicting the global environmental distribution of plastic polymers. *Environ. pollut.* 300, 118966. doi: 10.1016/j.envpol.2022.118966

Hu, M., and Palić, D. (2020). Micro- and nano-plastics activation of oxidative and inflammatory adverse outcome pathways. *Redox Biol.* 37, 101620. doi: 10.1016/j.redox.2020.101620

Hui, M., Liu, Y., Song, C., Li, Y., Shi, G., and Cui, Z. (2014). Transcriptome changes in *Eriocheir sinensis* megalopae after desalination provide insights into osmoregulation and stress adaption in larvae. *PloS One* 9, e114187. doi: 10.1371/journal.pone.0114187

Jia, Y., Wang, Z., Li, M., Jing, Q., Huang, B., Zhai, J., et al. (2020). Altered hepatic glycolysis, lipogenesis, and blood biochemistry of tiger puffer (*Takifugu rubripes*) under two different culture systems. *Aquaculture* 528, 735532. doi: 10.1016/j.aquaculture.2020.735532

Kanak, E. G., Dogan, Z., Eroglu, A., Atli, G., and Canli, M. (2014). Effects of fish size on the response of antioxidant systems of oreochromis niloticus following metal exposures. *Fish Physiol. Biochem.* 40, 1083–1091. doi: 10.1007/s10695-014-9907-x

Lee, W. S., Cho, H., Kim, E., Huh, Y. H., Kim, H., Kim, B., et al. (2019). Bioaccumulation of polystyrene nanoplastics and their effect on the toxicity of au ions in zebrafish embryos. *Nanoscale* 11, 3173–3185. doi: 10.1039/C8NR09321K

Lee, J. A., Marsden, I. D., and Glover, C. N. (2010). The influence of salinity on copper accumulation and its toxic effects in estuarine animals with differing osmoregulatory strategies. *Aquat Toxicol.* 99, 65–72. doi: 10.1016/j.aquatox.2010.04.006

Li, Z., Feng, C., Wu, Y., and Guo, X. (2020). Impacts of nanoplastics on bivalve: fluorescence tracing of organ accumulation, oxidative stress and damage. *J. Hazard Mater.* 392, 122418. doi: 10.1016/j.jhazmat.2020.122418

Li, Y., Ye, Y., Zhu, X., Liu, X., Li, X., Zhao, Y., et al. (2024). Transcriptomic analysis reveals nanoplastics-induced apoptosis, autophagy and immune response in *Litopenaeus vannamei*. *Sci. Total Environ.* 946, 174360. doi: 10.1016/j.scitotenv.2024.174360

Liu, P., Sun, S., Ai, Y., Feng, X., Zheng, Y., Gao, Y., et al. (2022). Elevated nuclear localization of glycolytic enzyme TPI1 promotes lung adenocarcinoma and enhances chemoresistance. *Cell Death Dis.* 13, 205. doi: 10.1038/s41419-022-04655-6

Liu, C., Wang, R., Gao, H., Wu, X., and Yin, D. (2022). Transport of trace metals and their bioaccumulation in zooplankton from changjiang (Yangtze river) to the east China sea. *Sci. Total Environ.* 851, 158156. doi: 10.1016/j.scitotenv.2022.158156

Liu, Y., Wang, J., Wei, Y., Zhang, H., Xu, M., and Dai, J. (2008). Induction of time-dependent oxidative stress and related transcriptional effects of perfluorododecanoic acid in zebrafish liver. *Aquat Toxicol.* 89, 242–250. doi: 10.1016/j.aquatox.2008.07.009

Liu, D., Yan, B., Yang, J., Lei, W., and Wang, L. (2011). Mitochondrial pathway of apoptosis in the hepatopancreas of the freshwater crab *Sinopotamon yangtsekiense* exposed to cadmium. *Aquat Toxicol.* 105, 394–402. doi: 10.1016/j.aquatox.2011.07.013

Liu, Z., Yu, P., Cai, M., Wu, D., Zhang, M., Chen, M., et al. (2019). Effects of microplastics on the innate immunity and intestinal microflora of juvenile *Eriocheir sinensis*. *Sci. Total Environ.* 685, 836–846. doi: 10.1016/j.scitotenv.2019.06.265

Livak, K. J., and Schmittgen, T. D. (2001). Analysis of relative gene expression data using real-time quantitative PCR and the $2^{-\Delta\Delta CT}$ method. *Methods* 25, 402–408. doi: 10.1006/meth.2001.1262

López, A. D. F., Fabiani, M., Lassalle, V. L., Spetter, C. V., and Severini, M. D. F. (2022). Critical review of the characteristics, interactions, and toxicity of micro/nanomaterials pollutants in aquatic environments. *Mar. pollut. Bull.* 174, 113276. doi: 10.1016/j.marpolbul.2021.113276

Lu, K., Qiao, R., An, H., and Zhang, Y. (2018). Influence of microplastics on the accumulation and chronic toxic effects of cadmium in zebrafish (*Danio rerio*). *Chemosphere* 202, 514–520. doi: 10.1016/j.chemosphere.2018.03.145

Luo, J., Zhu, T., Wang, X., Cheng, X., Yuan, Y., Jin, M., et al. (2020). Toxicological mechanism of excessive copper supplementation: effects on coloration, copper bioaccumulation and oxidation resistance in mud crab *Scylla paramamosain*. *J. Hazard Mater.* 395, 122600. doi: 10.1016/j.jhazmat.2020.122600

Manabe, M., Tatarazako, N., and Kinoshita, M. (2011). Uptake, excretion and toxicity of nano-sized latex particles on medaka (*Oryzias latipes*) embryos and larvae. *Aquat Toxicol.* 105, 576–581. doi: 10.1016/j.aquatox.2011.08.020

Nicholson, D. W. (1999). Caspase structure, proteolytic substrates, and function during apoptotic cell death. *Cell Death Differ.* 6, 1028–1042. doi: 10.1038/sj.cdd.4400598

Ortega, P., Custódio, M. R., and Zanotto, F. P. (2017). Characterization of cadmium transport in hepatopancreatic cells of a mangrove crab *Ucides cordatus*: the role of calcium. *Aquat Toxicol.* 188, 92–99. doi: 10.1016/j.aquatox.2017.04.012

Pacheco, A., Martins, A., and Guilhermino, L. (2018). Toxicological interactions induced by chronic exposure to gold nanoparticles and microplastics mixtures in *Daphnia magna*. *Sci. Total Environ.* 628-629, 474–483. doi: 10.1016/j.scitotenv.2018.02.081

Pan, Y., Qian, J., Ma, X., Huang, W., Fang, J. K., Arif, I., et al. (2023). Response of moulting genes and gut microbiome to nano-plastics and copper in juvenile horseshoe crab *Tachypleus tridentatus*. *Mar. Environ. Res.* 191, 106128. doi: 10.1016/j.marenvres.2023.106128

Qin, Z., Wang, S., Wu, Y., Sun, J., and Zhao, F. (2024). Seasonal dynamics of intestinal microbiota in juvenile chinese mitten crab (*Eriocheir sinensis*) in the yangtze estuary. *Front. Cell. Infect. Microbiol.* 14. doi: 10.3389/fcimb.2024.1436547

Ren, F., Jiang, H., Sun, J., He, L., Li, W., Wang, Y., et al. (2011). Cloning, characterization, expression, and copper sensitivity of the metallothionein-1 gene in

the chinese mitten crab, *Eriocheir sinensis*. *Mol. Biol. Rep.* 38, 2383–2393. doi: 10.1007/s11033-010-0372-z

Rodrigues, S., Antunes, S. C., Correia, A. T., and Nunes, B. (2011). Ecotoxicological evaluation of gilthead seabream (Sparus aurata) exposed to the antibiotic oxytetracycline using a multibiomarker approach. *Mar. Environ. Res.* 141, 233–246. doi: 10.1016/j.marenvres.2018.09.009

Santos, D., Luzio, A., Félix, L., Bellas, J., and Monteiro, S. M. (2022). Oxidative stress, apoptosis and serotonergic system changes in zebrafish (*Danio rerio*) gills after long-term exposure to microplastics and copper. *Comp. Biochem. Physiol. Part C: Toxicol. Pharmacol.* 258, 109363. doi: 10.1016/j.cbpc.2022.109363

Shen, C., Feng, G., Zhao, F., Huang, X., Wang, M., and Wang, H. (2023a). Integration of transcriptomics and proteomics analysis reveals the molecular mechanism of *Eriocheir sinensis* gills exposed to heat stress. *Antioxidants* 12, 2020. doi: 10.3390/antiox12122020

Shen, C., Wang, R., Feng, G., Zhuang, P., Zhang, T., and Huang, X. (2023b). Correlation analysis of migration in *Eriocheir sinensis* of the yangtze river estuary based on salinity preference. *Environ. Sci. pollut. Res.* 30, 10724–10732. doi: 10.1007/s11356-022-22850-y

Shen, M., Zhang, Y., Zhu, Y., Song, B., Zeng, G., Hu, D., et al. (2019). Recent advances in toxicological research of nanoplastics in the environment: a review. *Environ. pollut.* 252, 511–521. doi: 10.1016/j.envpol.2019.05.102

Shukla, S., Khan, R., Saxena, A., and Sekar, S. (2022). Microplastics from face masks: a potential hazard post covid-19 pandemic. *Chemosphere* 302, 134805. doi: 10.1016/j.chemosphere.2022.134805

Silvestre, F., Trausch, G., and Devos, P. (2005). Hyper-osmoregulatory capacity of the chinese mitten crab (*Eriocheir sinensis*) exposed to cadmium; Acclimation during chronic exposure. *Comp. Biochem. Physiol. Part C: Toxicol. Pharmacol.* 140, 29–37. doi: 10.1016/j.cca.2004.12.007

Sonnack, L., Kampe, S., Muth-Köhne, E., Erdinger, L., Henny, N., Hollert, H., et al. (2015). Effects of metal exposure on motor neuron development, neuromasts and the escape response of zebrafish embryos. *Neurotoxicol Teratol* 50, 33–42. doi: 10.1016/j.ntt.2015.05.006

Tang, D., Liu, R., Shi, X., Shen, C., Bai, Y., Tang, B., et al. (2021). Toxic effects of metal copper stress on immunity, metabolism and pathologic changes in chinese mitten crab (*Eriocheir japonica sinensis*). *Ecotoxicology* 30, 632–642. doi: 10.1007/s10646-021-02367-9

Tian, L., Chen, Q., Jiang, W., Wang, L., Xie, H., Kalogerakis, N., et al. (2019). A carbon-14 radiotracer-based study on the phototransformation of polystyrene nanoplastics in water versus in air. *Environ. science Nano* 6, 2907–2917. doi: 10.1039/C9EN00662A

Turan, N. B., Erkan, H. S., Engin, G. O., and Bilgili, M. S. (2019). Nanoparticles in the aquatic environment: usage, properties, transformation and toxicity—a review. *Process Saf Environ. Protect* 130, 238–249. doi: 10.1016/j.psep.2019.08.014

Valencia-Castañeda, G., Frías-Espericueta, M. G., Vanegas-Pérez, R. C., Chávez-Sánchez, M. C., and Páez-Osuna, F. (2020). Physiological changes in the hemolymph of juvenile shrimp *Litopenaeus vannamei* to sublethal nitrite and nitrate stress in low-salinity waters. *Environ. Toxicol. Pharmacol.* 80, 103472. doi: 10.1016/j.etap.2020.103472

Varó, I., Perini, A., Torreblanca, A., Garcia, Y., Bergami, E., Vannuccini, M. L., et al. (2019). Time-dependent effects of polystyrene nanoparticles in brine shrimp *Artemia franciscana* at physiological, biochemical and molecular levels. *Sci. Total Environ.* 675, 570–580. doi: 10.1016/j.scitotenv.2019.04.157

Wang, Z., Guan, Y., Wang, Y., Zhu, S., Cui, C., and Wang, X. (2023). Transcriptome and histopathology analyses of the gills of *Eriocheir sinensis* provide novel insights into the molecular mechanism of pb stress. *Aquac Int.* 31, 3329–3344. doi: 10.1007/s10499-023-01126-3

Wei, W., Yang, Q., Xiang, D., Chen, X., Wen, Z., Wang, X., et al. (2023). Combined impacts of microplastics and cadmium on the liver function, immune response, and intestinal microbiota of crucian carp (*Carassius carassius*). *Ecotoxicol Environ. Saf* 261, 115104. doi: 10.1016/j.ecoenv.2023.115104

Xing, Y., Feng, Y., Tian, J., Zhang, Y., Han, C., Liu, X., et al. (2025). Nitrite and sulfide stress affects physiological and metabolic functions of gills in crab *Eriocheir sinensis*. *Aquaculture* 594, 741437. doi: 10.1016/j.aquaculture.2024.741437

Yang, X., Shi, X., Wu, M., Pang, Y., Song, X., Shi, A., et al. (2021). Effects of melatonin feed on histology and antioxidant ability of the gills and oxygen consumption of chinese mitten crab (*Eriocheir sinensis*), exposed to acute hypoxia stress. *Aquaculture* 544, 737015. doi: 10.1016/j.aquaculture.2021.737015

Yang, Z., Zhao, Y., Li, N., Yang, J., and Hua, X. (2008). Effects of water-borne copper on the y-organ and content of 20-hydroxyecdysone in *Eriocheir sinensis*. *Arch. Environ. Contam Toxicol.* 54, 69–74. doi: 10.1007/s00244-007-9007-3

Yang, Z., Zhu, L., Liu, J., Cheng, Y., Waiho, K., Chen, A., et al. (2022). Polystyrene microplastics increase pb bioaccumulation and health damage in the chinese mitten crab *Eriocheir sinensis*. *Sci. Total Environ.* 829, 154586. doi: 10.1016/j.scitotenv.2022.154586

Yu, F., Pei, Y., Zhang, X., Wu, X., Zhang, G., and Ma, J. (2023). Occurrence and distribution characteristics of aged microplastics in the surface water, sediment, and crabs of the aquaculture pond in the yangtze river delta of China. *Sci. Total Environ.* 871, 162039. doi: 10.1016/j.scitotenv.2023.162039

Zarfl, C., and Matthies, M. (2010). Are marine plastic particles transport vectors for organic pollutants to the arctic? *Mar. pollut. Bull.* 60, 1810–1814. doi: 10.1016/j.marpolbul.2010.05.026

Zeng, L., Zheng, J., Wang, Y., Xu, M., Zhu, A., and Wu, C. (2016). The role of nrf2/keap1 signaling in inorganic mercury induced oxidative stress in the liver of large yellow croaker pseudosciaena crocea *Pseudosciaena crocea*. *Ecotoxicol Environ. Saf* 132, 345–352. doi: 10.1016/j.ecoenv.2016.05.002

Zhang, T., Du, N., Geng, Z., Wang, S., Gao, Y., Yang, G., et al. (2023). Estimation of estuarine habitat degradation and its influence on the reproduction process of the crab *Eriocheir sinensis* in the yangtze river estuary. *Ecol. Process* 12 (1), 59. doi: 10.1186/s13717-023-00473-6

Zhang, Y., Gao, G., Lin, R., Aweya, J. J., Tao, M., and Wang, F. (2018). Transcriptome analyses reveal *Litopenaeus vannamei* hemocytes response to lipopolysaccharide. *Fish Shellfish Immunol.* 76, 187–195. doi: 10.1016/j.fsi.2018.03.002

Zhang, F., Li, D., Yang, Y., Zhang, H., Zhu, J., Liu, J., et al. (2022). Combined effects of polystyrene microplastics and copper on antioxidant capacity, immune response and intestinal microbiota of nile tilapia (*Oreochromis niloticus*). *Sci. Total Environ.* 808, 152099. doi: 10.1016/j.scitotenv.2021.152099

Zhang, C., Ye, L., Wang, C., Xiong, X., Li, Y., Li, P., et al. (2022). Toxic effect of combined exposure of microplastics and copper on goldfish (*Carassius auratus*): insight from oxidative stress, inflammation, apoptosis and autophagy in hepatopancreas and intestine. *Bull. Environ. Contam Toxicol.* 109, 1029–1036. doi: 10.1007/s00128-022-03585-5

Zhao, X., Yang, Z., and Cheng, Y. (2021). Effects of cadmium alone and in combination with ph on bioaccumulation, tissue structure, and enzyme activity of the chinese mitten crab, *Eriocheir sinensis*. *Comp. Biochem. Physiol. Part C: Toxicol. Pharmacol.* 245, 109025. doi: 10.1016/j.cbpc.2021.109025

Zhao, S., Zhu, L., Wang, T., and Li, D. (2014). Suspended microplastics in the surface water of the yangtze estuary system, China: first observations on occurrence, distribution. *Mar. pollut. Bull.* 86, 562–568. doi: 10.1016/j.marpolbul.2014.06.032

Zhu, J., Miao, G., Jiang, H., Su, H., Wang, Y., Chen, L., et al. (2024). Polystyrene nanoplastics at predicted environmental concentrations enhance the toxicity of copper on *Caenorhabditis elegans*. *Ecotoxicol Environ. Saf* 282, 116749. doi: 10.1016/j.ecoenv.2024.116749